Supporting Information

Thermodynamic Screening of Metal Substituted MOFs for Carbon Capture

Hyun Seung Koh,[†] Malay Kumar Rana,[†] Jinhyung Hwang,[†] and Donald J. Siegel[*,†]

[†]Mechanical Engineering Department, University of Michigan, Ann Arbor, Michigan 48109, United States.

Contents

Table S1. Calculated cell parameters and cell volumes for M-DOBDC and M-HKUST-1 systems compared to experiments.

MOF	Metal	a (Å)	c (Å)	V (Å^3)	Experiment		
					a (Å)	c (Å)	V (Å^3)
DOBDC	Be	26.29	6.32	3780.72			
	Mg	26.12	6.93	4097.08	26.02[1]	6.72[1]	3940.75[1]
	Ca	26.54	7.69	4690.18			
	Sr	26.13	8.08	4779.14			
	Sc	26.11	7.25	4280.02			
	Ti	26.39	6.99	4212.88			
	V	26.07	6.97	4104.92			
	Cr	26.00	6.94	4064.92			
	Mn	26.35	7.15	4297.38	26.23[2]	7.04[2]	
	Fe	26.36	6.88	4142.66	26.10[3]	6.85[3]	4041.30[3]
	Co	26.16	6.89	3967.10	26.11[4]	6.72[4]	
	Ni	25.89	6.79	3898.34	25.79[5]	6.77[5]	3898.34[5]
	Cu	25.60	6.70	3806.73	26.00[6]	6.26[6]	3663.3[6]
	Zn	26.17	6.92	4102.34	25.93[7]	6.83[7]	
	Mo	26.22	7.00	4168.57			
	Sn	26.62	7.19	4411.11			
	W	26.98	6.29	3964.40			
	Pb	26.65	8.05	4948.50			
HKUST-1	Be	25.42		16428.72			
	Mg	26.62		18853.14			
	Ca	27.36		20480.62			
	Sr	27.72		21309.72			
	Sc	26.62		18867.43			
	Ti	26.68		18992.96			
	V	26.73		19091.71			
	Cr	26.70		19028.93	26.67[8]		18959.88[8]
	Mn	26.38		18352.21			
	Fe	26.35		18303.91			
	Co	26.21		18025.33			
	Ni	26.31		18219.00	26.59[9]		18808.57[9]
	Cu	26.48		18572.70	26.34[10]		18280.00[10]
	Zn	26.82		19286.58	26.52[11]		18651.79[11]
	Mo	27.30		20337.12	27.13[12]		19966.47[12]
	Sn	27.03		19741.74			
	W	27.19		20096.96			
	Pb	27.64		21106.10			

Table S2. Average calculated metal-oxygen bond lengths (in Å) within M-DOBDC. In all cases the metal ion adopts either a tetragonal or square pyramidal coordination to oxygen; a missing value for d(M-05) indicates that the structure adopts a tetrahedral geometry.

MOFs	Metal	d(M-O1)	d(M-O2)	d(M-O3)	d(M-O4)	d(M-O5)
DOBDC	Be	1.54	1.622	1.681	1.756	
	Mg	2.032	2.032	2.045	2.048	2.087
	Ca	2.284	2.304	2.326	2.352	2.375
	Sr	2.436	2.468	2.535	2.536	2.549
	Sc	2.105	2.221	2.03	2.109	2.205
	Ti	2.059	2.061	2.013	2.081	1.963
	V	2.033	2.059	2.102	2.025	2.07
	Cr	2.002	2.033	2.038	2.079	
	Mn	2.088	2.103	2.107	2.145	2.264
	Fe	2.045	2.072	2.074	2.128	2.156
	Co	2.003	2.026	2.065	2.074	2.123
	Ni	1.986	2.023	2.023	2.102	2.108
	Cu	1.974	1.988	1.999	2.056	
	Zn	2.033	2.045	2.052	2.101	2.195
	Mo	2.073	2.106	2.169	2.179	2.187
	W	2.047	2.05	2.175	2.216	2.217
	Sn	2.291	2.313	2.328	2.34	
	Pb	2.328	2.388	2.554	2.611	2.696

Table S3. Average calculated metal-oxygen and metal-metal bond lengths (in Å) for M-HKUST-1. The SBUs in M-HKUST-1s exhibit a paddle wheel geometry, with 4 metal-oxygen bonds and one metal-metal bond.

MOFs	Metal	d(M-O1)	d(M-O2)	d(M-O3)	d(M-O4)	d(M-M)
HKUST-1	Be	1.738	1.738	1.73	1.73	2.469
	Mg	2.008	2.008	2.008	2.008	2.937
	Ca	2.254	2.254	2.254	2.254	3.61
	Sr	2.41	2.41	2.41	2.41	3.895
	Sc	2.079	2.079	2.079	2.079	3.151
	Ti	1.973	1.973	1.973	1.973	2.872
	V	2.037	2.037	2.037	2.037	1.97
	Cr	1.99	1.99	1.99	1.99	2.086
	Mn	1.936	1.936	1.936	1.936	2.578
	Fe	1.925	1.925	1.925	1.925	2.201
	Co	1.908	1.908	1.908	1.908	2.235
	Ni	1.938	1.938	1.938	1.938	2.351
	Cu	1.975	1.975	1.975	1.975	2.521
	Zn	2.032	2.032	2.032	2.032	2.644
	Mo	2.1	2.1	2.101	2.101	2.136
	W	2.077	2.077	2.077	2.077	2.214
	Sn	2.265	2.265	2.293	2.293	4.199
	Pb	2.38	2.38	2.379	2.379	4.212

Table S4. Tabulated ionic radii of +2 metal ions[13] and electronegativity of the metal atoms[14]. Low spin configurations refer to metals in M-DOBDC; high spin cases refer to M-HKUST-1.

Metal	Radii (Å)		Electro-negativity
	Low spin	High spin	
Be	0.45		1.57
Mg	0.72		1.31
Ca	1.00		1
Sr	1.18		0.95
Sc			1.36
Ti	0.86		1.54
V	0.79		1.63
Cr	0.73	0.80	1.66
Mn	0.67	0.83	1.55
Fe	0.61	0.78	1.83
Co	0.65	0.745	1.88
Ni	0.69		1.91
Cu	0.73		1.9
Zn	0.74		1.65
Mo			2.16
W			2.36
Sn	0.93[15]		1.96
Pb	1.19		2.33

Table S5. Calculated bond lengths (Å) and bond angles **(°)** involving the MOF metal site (M) and adsorbed CO_2. d(M-O) refers to the distance between the metal and the nearest oxygen in CO_2; d(MO-CO) is the length of the O-C bond (within CO_2) closest to the metal; d(C-O) is the length of the O-C bond (within CO_2) farthest from the metal;<M-O-C is the angle formed by the metal and the nearest O and C in CO_2; <O-C-O is bending angle within the CO_2 molecule.

MOF	Metal	d(M-O)	d(MO-CO)	d(C-O)	<M-O-C	<O-C-O
M/DOBDC	Be	3.858	1.181	1.179	84.261	180.000
	Mg	2.392	1.184	1.174	130.950	178.350
	Ca	2.623	1.182	1.174	148.845	178.599
	Sr	2.842	1.181	1.176	160.263	178.472
	Sc	2.445	1.187	1.172	135.160	176.462
	Ti	2.444	1.186	1.173	131.538	177.235
	V	2.340	1.185	1.173	133.553	177.738
	Cr	3.286	1.182	1.179	110.796	180.000
	Mn	2.695	1.183	1.176	125.079	180.000
	Fe	2.717	1.183	1.177	119.707	179.141
	Co	2.812	1.183	1.177	115.950	179.053
	Ni	2.617	1.183	1.176	120.292	179.016
	Cu	3.228	1.181	1.179	109.914	180.000
	Zn	2.867	1.183	1.177	115.937	178.883
	Mo	2.528	1.185	1.174	128.753	178.437
	W	2.450	1.187	1.173	132.420	178.262
	Sn	4.007	1.180	1.180	84.521	180.000
	Pb	3.402	1.182	1.178	131.434	180.000
M/HKUST-1	Be	1.945	1.190	1.169	118.703	177.382
	Mg	2.221	1.191	1.168	117.588	177.245
	Ca	2.624	1.188	1.170	111.801	177.425
	Sr	2.861	1.187	1.172	108.801	177.576
	Sc	2.096	1.290	1.204	88.769	140.807
	Ti	2.686	1.189	1.172	111.964	180.000
	V	2.772	1.186	1.174	110.961	180.000
	Cr	3.149	1.182	1.177	101.390	180.000
	Mn	3.106	1.182	1.177	100.034	180.000
	Fe	3.282	1.180	1.179	96.000	180.000
	Co	2.584	1.185	1.175	112.243	180.000
	Ni	2.731	1.184	1.176	107.581	180.000
	Cu	2.769	1.184	1.176	106.633	180.000
	Zn	2.384	1.188	1.171	116.371	178.106
	Mo	3.340	1.182	1.178	100.457	180.000
	W	3.127	1.184	1.176	105.326	180.000
	Sn	3.811	1.177	1.181	79.773	180.000
	Pb	3.840	1.182	1.178	73.975	180.000

Table S6. Calculated binding energies (ΔE) at 0K, zero point energies (ZPE), thermal energy contributions (TE) at 300K, and adsorption enthalpies (ΔH) at 300K for M-DOBDC and M-HKUST-1 within the LDA, PBE-GGA, DFT-D2 and revPBE-vdW methods. All energies are given in kJ/mol CO_2. rPBE-vdW is shorthand for revPBE-vdW

		ΔE (kJ/mol)				ZPE (kJ/mol)		TE (kJ/mol)		ΔH (kJ/mol)		Exp
		LDA	PBE	DFT-D2	rPBE-vdW	DFT-D2	rPBE-vdW	DFT-D2	rPBE-vdW	DFT-D2	rPBE-vdW	
M-DOBDC	Be	-20.62	-9.71	-19.49	-34.01	2.88	1.38	1.04	0.82	-15.57	-31.81	
	Mg	-52.30	-27.06	-42.31	-50.89	2.36	2.15	1.40	1.53	-38.55	-47.20	-44.2±4.6
	Ca	-48.28	-28.67	-39.87	-50.21	2.30	2.03	1.44	1.93	-36.13	-46.26	
	Sr	-41.67	-25.50	-34.36	-46.88	2.64	1.35	1.35	0.91	-30.37	-44.63	
	Sc		-21.03	-43.85	-53.92	0.24	0.84	1.82	1.53	-41.79	-51.54	
	Ti	-69.16	-26.02	-51.23	-56.15	2.40	2.25	0.98	1.22	-47.85	-52.69	
	V	-52.61	-29.63	-54.13	-57.49	2.88	2.92	-0.94	1.11	-52.18	-53.46	
	Cr	-36.41	-10.94	-19.14	-36.68	1.73	1.53	-0.02	2.30	-17.43	-32.85	
	Mn	-37.06	-16.55	-28.56	-39.12	0.56	1.27	-0.91	0.59	-28.91	-37.25	
	Fe	-35.23	-9.54	-25.19	-33.67	2.55	1.27	-0.94	-0.01	-23.58	-32.40	
	Co	-39.38	-14.68	-29.88	-39.32	1.67	1.56	-0.73	0.52	-28.95	-37.24	-35.7±1.9
	Ni		-17.05	-33.62	-41.22	3.81	1.68	0.47	1.82	-29.35	-37.72	-39.6±1.5
	Cu	-30.70	-9.10	-19.14	-27.17	3.37	2.07	0.12	-0.04	-15.65	-25.14	-24
	Zn	-40.87	-16.51	-30.53	-40.99	1.16	1.52	-0.10	2.89	-29.47	-36.59	30.5+0.5
	Mo	-72.22	-29.32	-48.78	-50.05	1.27	3.05	0.24	1.08	-47.27	-45.93	
	W	-72.37	-31.11	-44.68	-48.92	1.71	2.95	1.40	0.85	-41.58	-45.12	
	Sn	-26.23	-7.52	-17.56	-26.95	3.82	1.43	-0.44	0.46	-14.18	-25.06	
	Pb	-26.09	-7.33	-13.14	-28.17	2.44	1.77	1.31	0.78	-9.39	-25.62	
M-HKUST-1	Be	-61.63	-29.04	-43.68	-48.09	2.34	3.12	0.04	-2.54	-41.30	-47.51	
	Mg	-59.50	-35.37	-52.27	-57.12	3.84	2.29	1.46	-1.32	-46.96	-56.14	
	Ca	-48.79	-25.15	-50.58	-51.41	2.71	1.80	-2.18	-1.69	-50.06	-51.30	
	Sr	-45.26	-20.85	-52.65	-51.78	2.88	7.70	3.92	-0.98	-45.85	-45.06	
	Sc	-57.40	-31.91	-42.91	-47.81	1.31	0.85	-2.02	2.16	-43.62	-44.80	
	Ti	-42.32	-13.59	-27.87	-29.90	0.33	1.61	-3.36	-2.33	-30.90	-30.62	
	V	-29.98	-2.81	-17.83	-18.72	0.08	1.22	-5.67	-0.40	-23.42	-17.89	
	Cr	-27.13	-7.59	-21.32	-24.85	2.39	2.01	-1.52	0.76	-20.44	-22.08	-26.7
	Mn	-26.10	-5.80	-21.14	-25.68	4.49	1.21	-4.22	-1.93	-20.87	-26.40	
	Fe	-30.47	-4.93	-19.95	-25.76	6.51	0.68	1.47	-1.44	-11.97	-26.52	
	Co	-43.66	-11.92	-26.37	-30.36	1.73	2.17	2.46	-0.72	-22.19	-28.91	
	Ni	-20.46	-9.59	-23.50	-28.45	0.90	1.09	-1.05	-4.95	-23.65	-32.31	-36.8
	Cu	-31.49	-8.93	-22.56	-27.32	4.81	0.94	-0.08	-4.09	-17.83	-30.47	-23.7±8.2
	Zn	-55.56	-25.37	-38.67	-41.08	2.64	3.58	1.65	0.94	-34.38	-36.56	
	Mo	-25.96	-6.40	-22.03	-25.55	1.88	1.35	2.65	-2.21	-17.50	-26.41	-25.6
	W	-26.32	-5.94	-21.48	-22.40	9.45	0.85	-3.90	2.16	-15.93	-19.39	
	Sn	-20.94	1.69	-9.04	-21.01	-2.33	1.61	-2.69	-2.33	-14.06	-21.74	
	Pb	-3.72	4.44	-7.31	-10.15	4.09	1.22	-1.86	-0.40	-5.07	-9.33	

Table S7. Change in the metal atom's (Δq_M) and CO_2 molecule's partial charge (Δq_{CO2}) upon CO_2 adsorption. $\Delta q < 0$ indicates a reduction in positive charge.

metal	DOBDC		HKUST-1	
	Δq_M	Δq_{CO2}	Δq_M	Δq_{CO2}
Sc	0.160	0.007	0.221	-0.314
Ti	-0.398	0.039	0.141	-0.002
V	-0.204	0.031	0.422	0.002
Cr	0.057	-0.037	0.055	0.001
Mn	0.171	-0.015	0.095	-0.001
Fe	-0.042	-0.019	0.062	0.000
Co	0.042	-0.021	-0.035	0.010
Ni	-0.035	-0.003	0.021	0.006
Cu	0.044	-0.016	0.117	0.006
Zn	0.072	-0.024	-0.140	0.051
Mo	-0.264	0.044	0.059	-0.006
W	-0.075	0.056	0.083	-0.003

Figure S1. *tran*-configuration of CO2 molecules in Cu-HKUST-1. (red = Oxygen, black = Carbon, blue = copper)

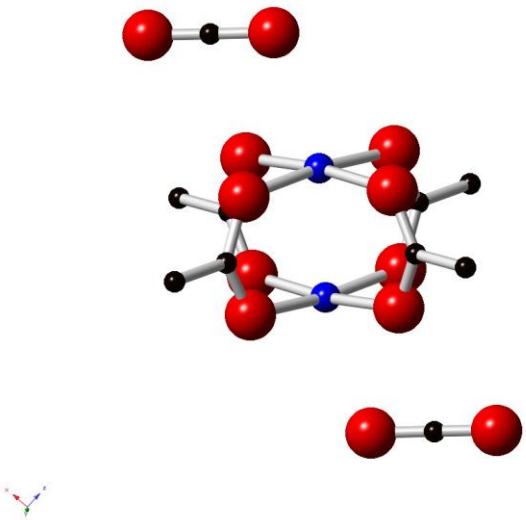

Figure S2. Calculated local geometries for the M-DOBDC SBU; for clarity, only a portion of the infinite SBU chain is included. Oxygen atoms are red, other colors represent metals. Numbers following the element name indicate the coordination of the metal site. Clusters highlighted in red (Be, Cr, Cu, Sn) exhibit tetrahedral bonding of the metal ions; yellow highlighting (Pb) indicates the presence of other significant structural distortions.

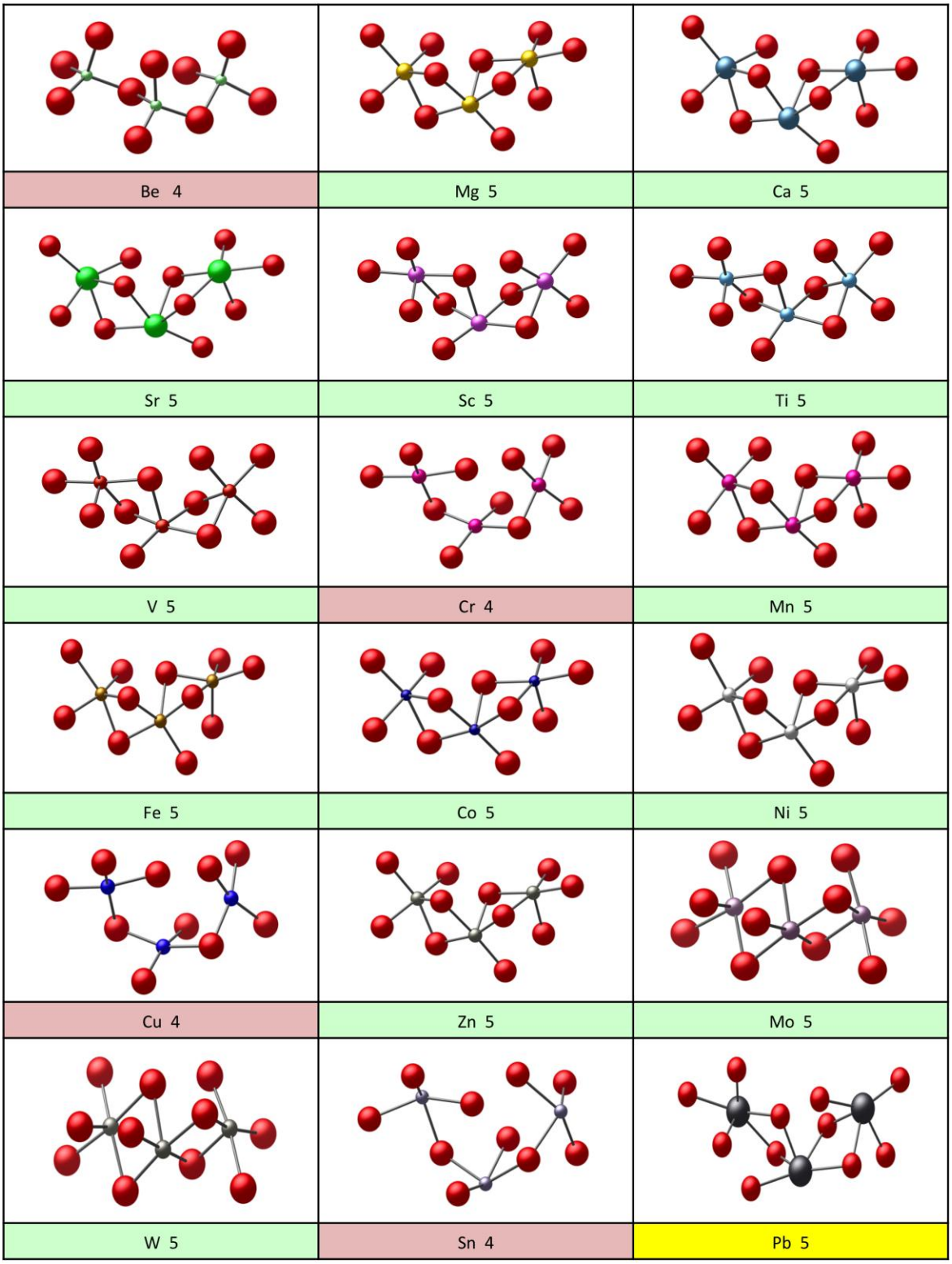

Figure S3. Calculated local geometries for the M-HKUST-1 SBU. Oxygen atoms are red, carbon is black, and other colors represent metals. Clusters highlighted in yellow (Ca, Sr, Sn, Pb) exhibit large distortions to the paddle-wheel structure.

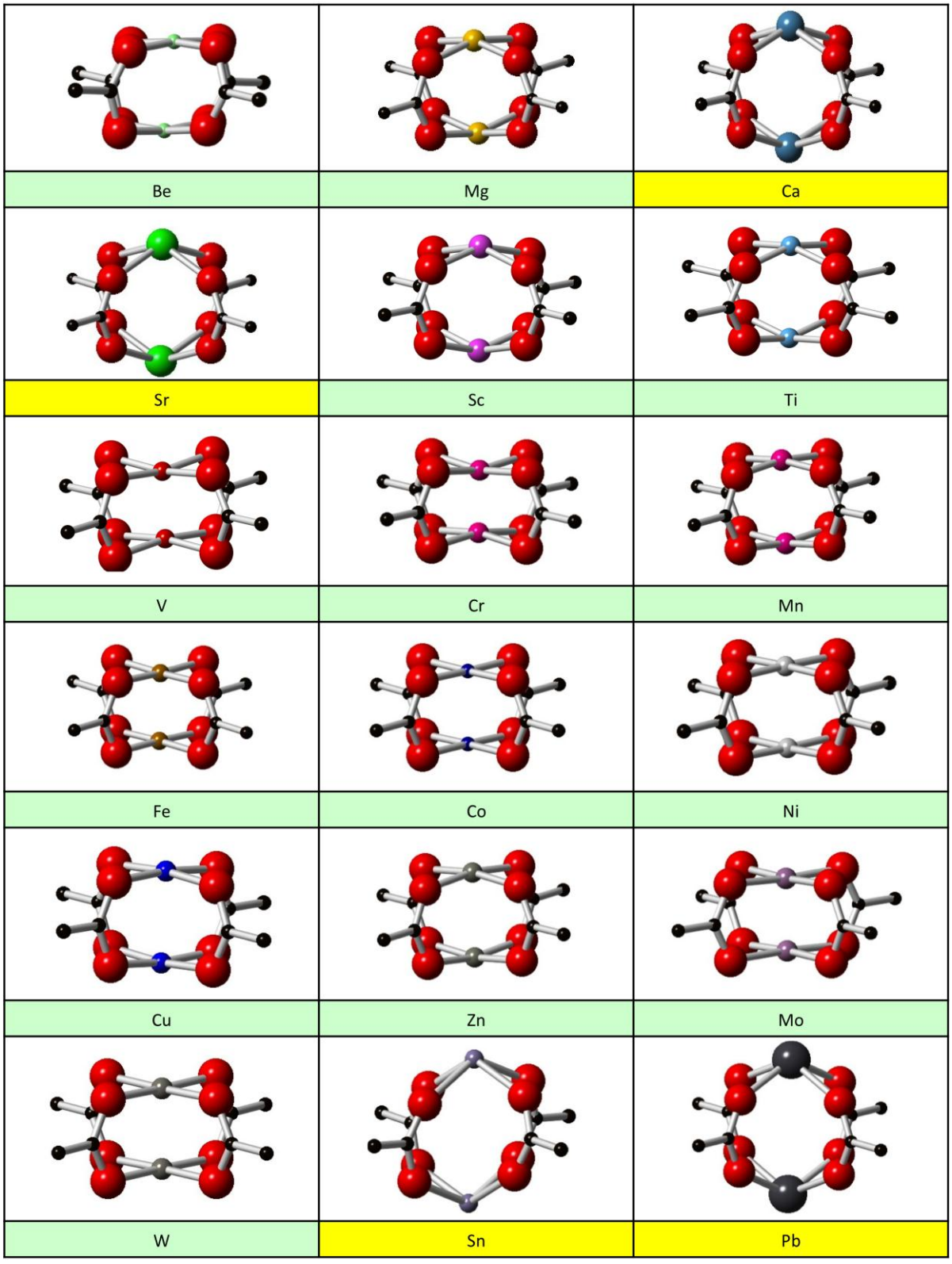

Figure S4. Charge density difference plots for M-DOBDC. Red and yellow indicate charge accumulation; blue indicates charge depletion. For clarity, only the CO_2 molecule, the metal, and the metal's nearest-neighbor oxygen atoms are illustrated.

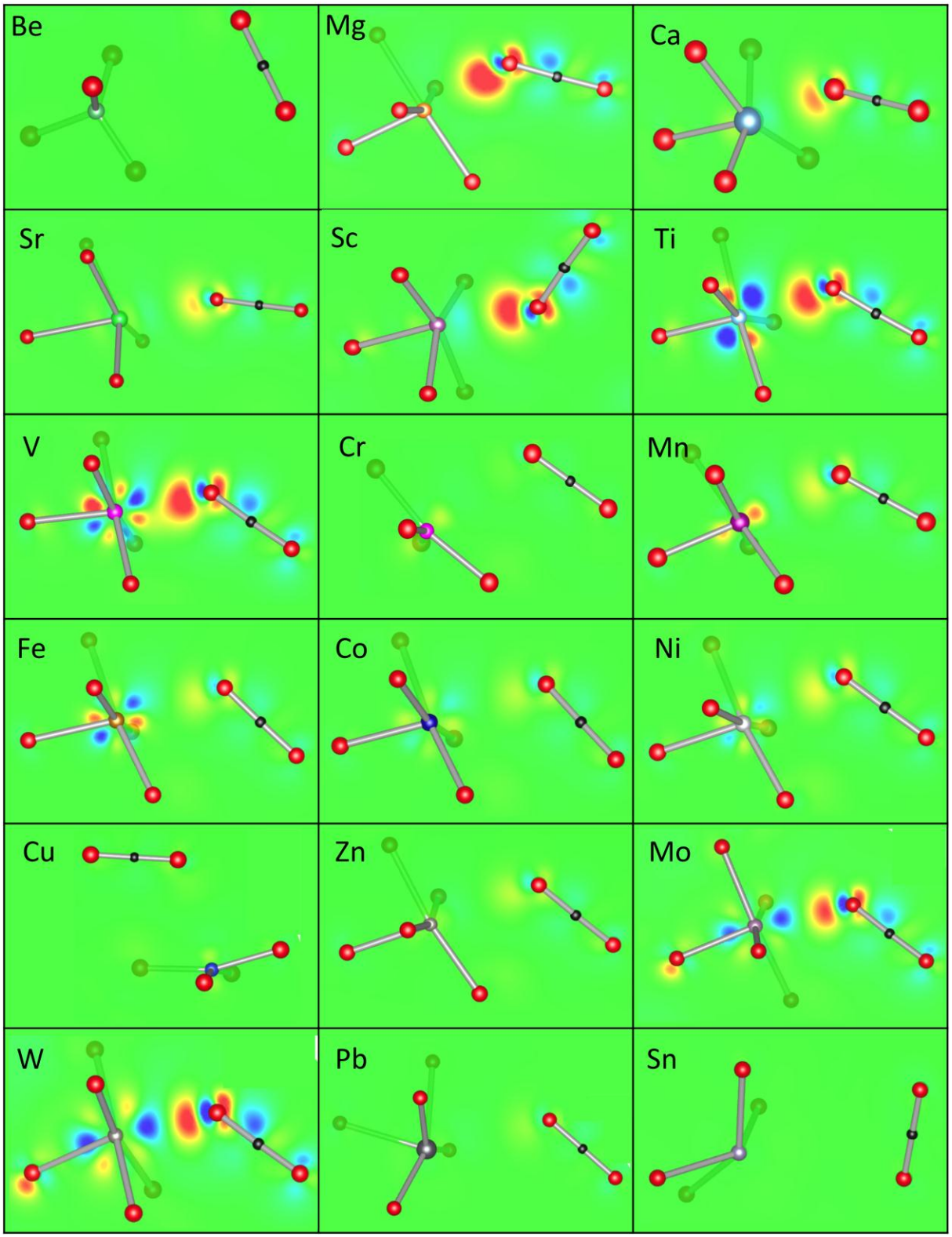

Figure S5. Charge density difference plots for M-HKUST-1. Red and yellow indicate charge accumulation; blue indicates charge depletion. For clarity, only the CO_2 molecules and atoms from the paddle-wheel SBU are illustrated.

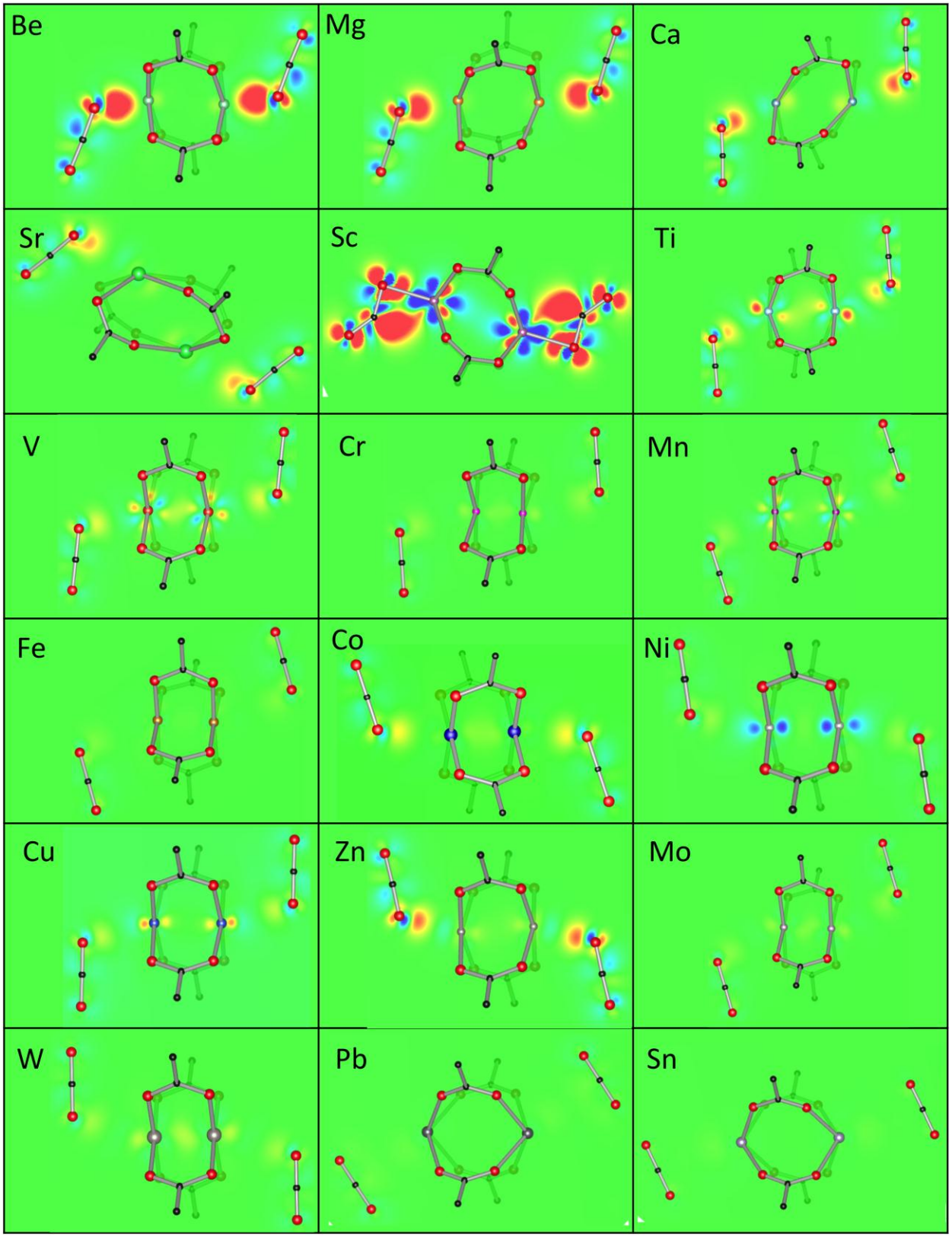

Figure S6. CO_2 and metal LDOS for M-DOBDC. (Be, Mg, Ca, Sr, Sc, Ti, V, Cr, and Mn)

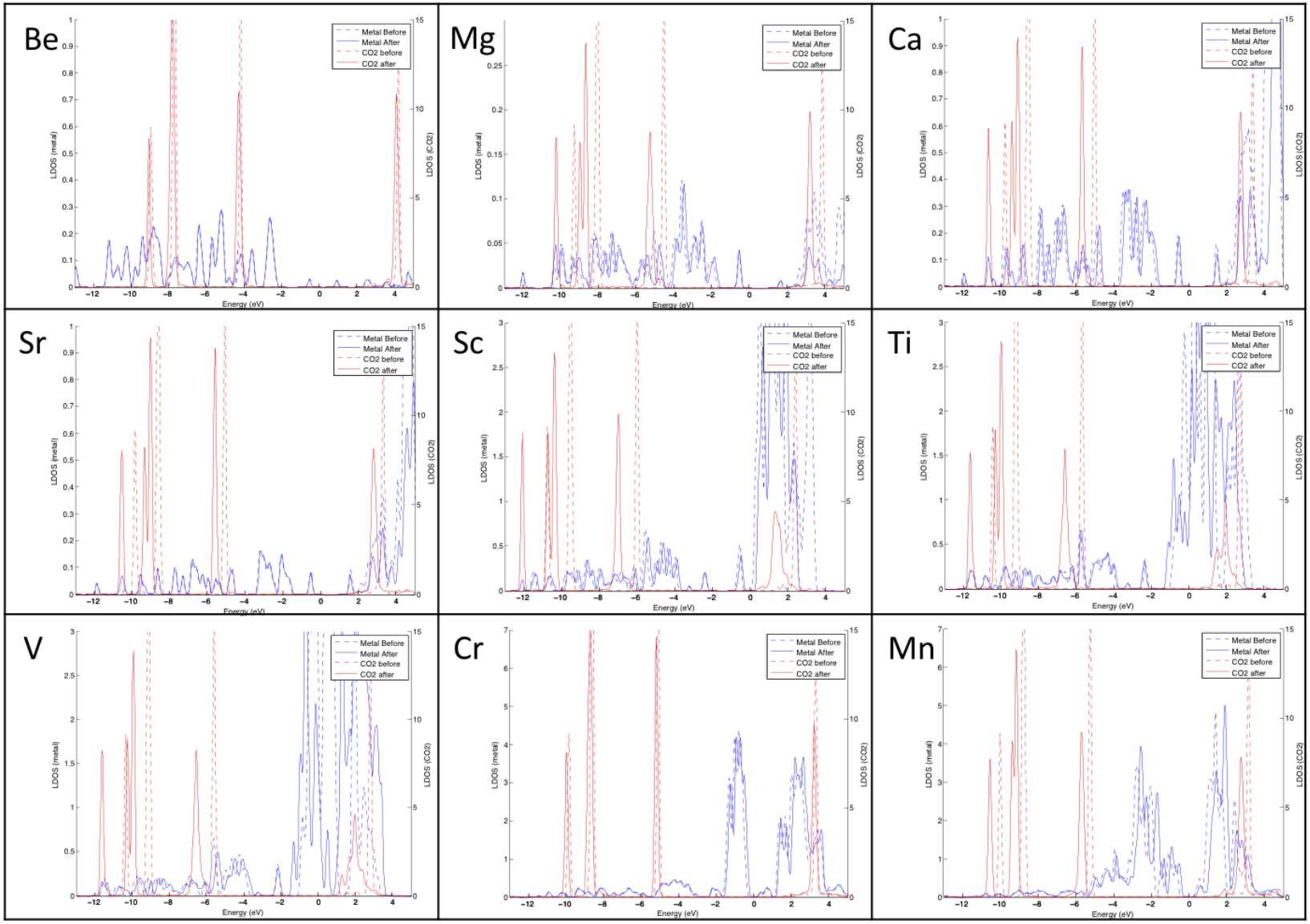

Figure S7. Figure S7. CO_2 and metal LDOS for M-DOBDC. (Fe, Co, Ni, Cu, Zn, Mo, W, Sn, and Pb)

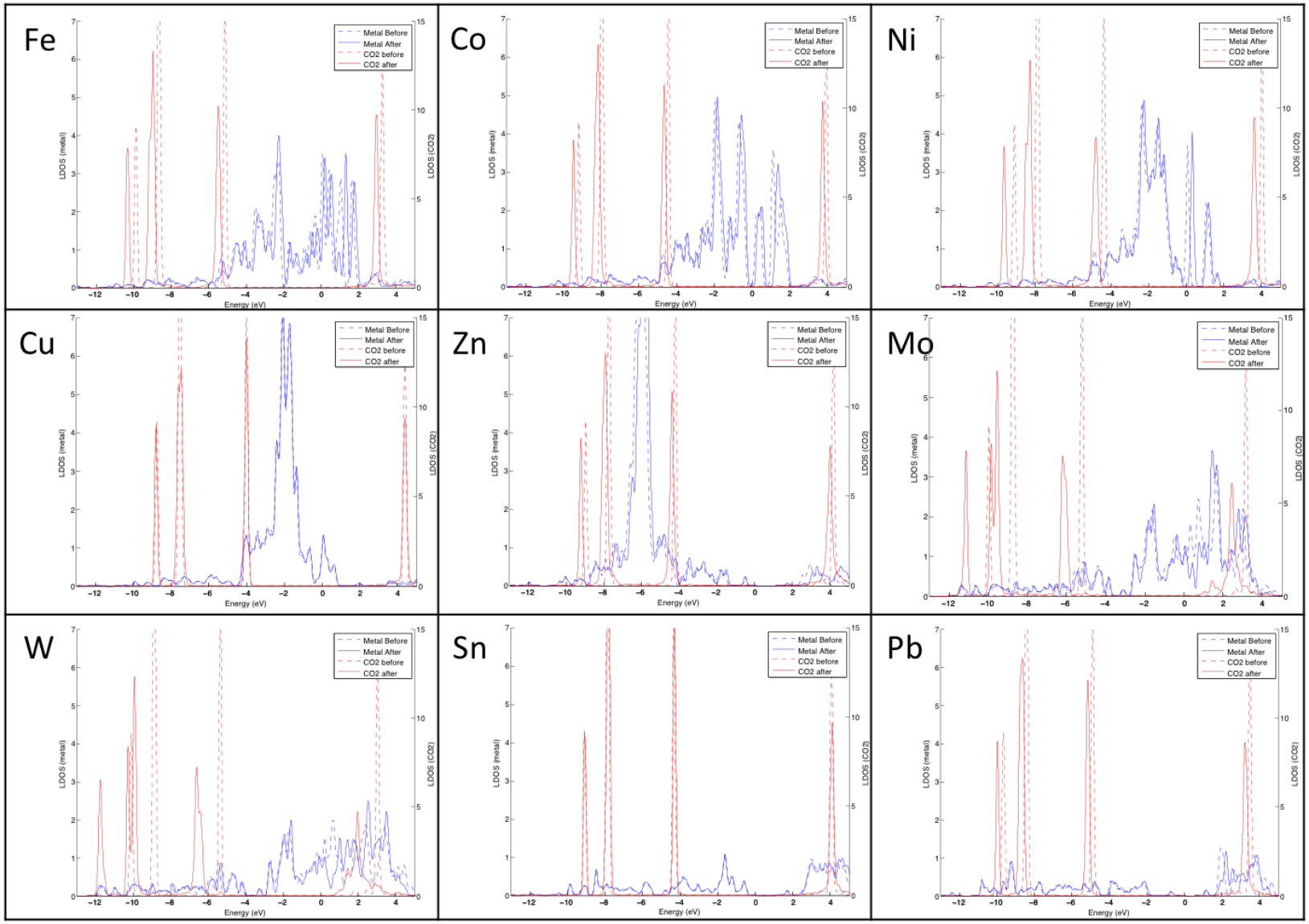

Figure S8. CO_2 and metal LDOS for M-HKSUT-1. (Be, Mg, Ca, Sr, Sc, Ti, V, Cr, and Mn)

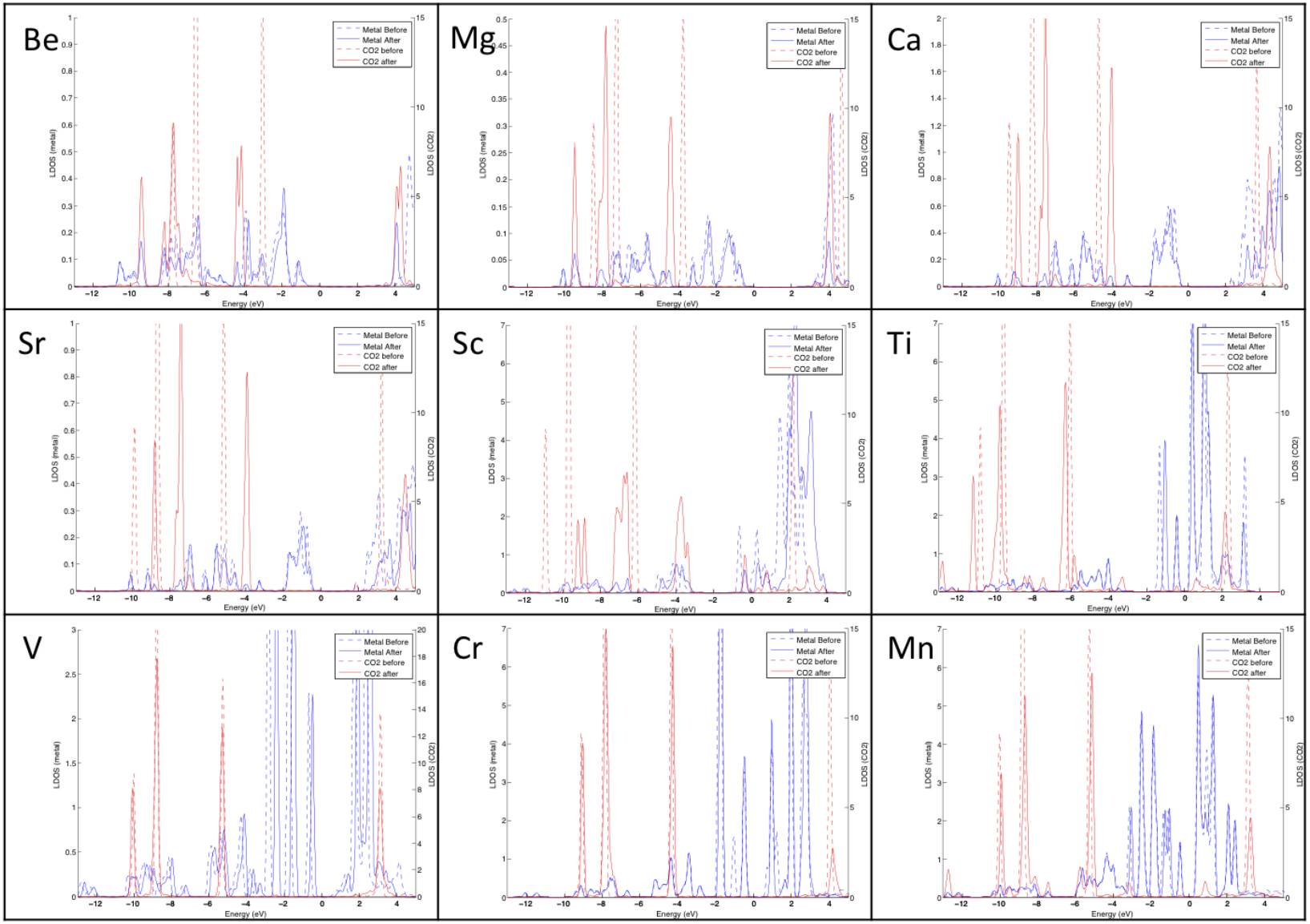

Figure S9. CO_2 and metal LDOS for M-HKSUT-1. (Fe, Co, Ni, Cu, Zn, Mo, W, Sn, and Pb)

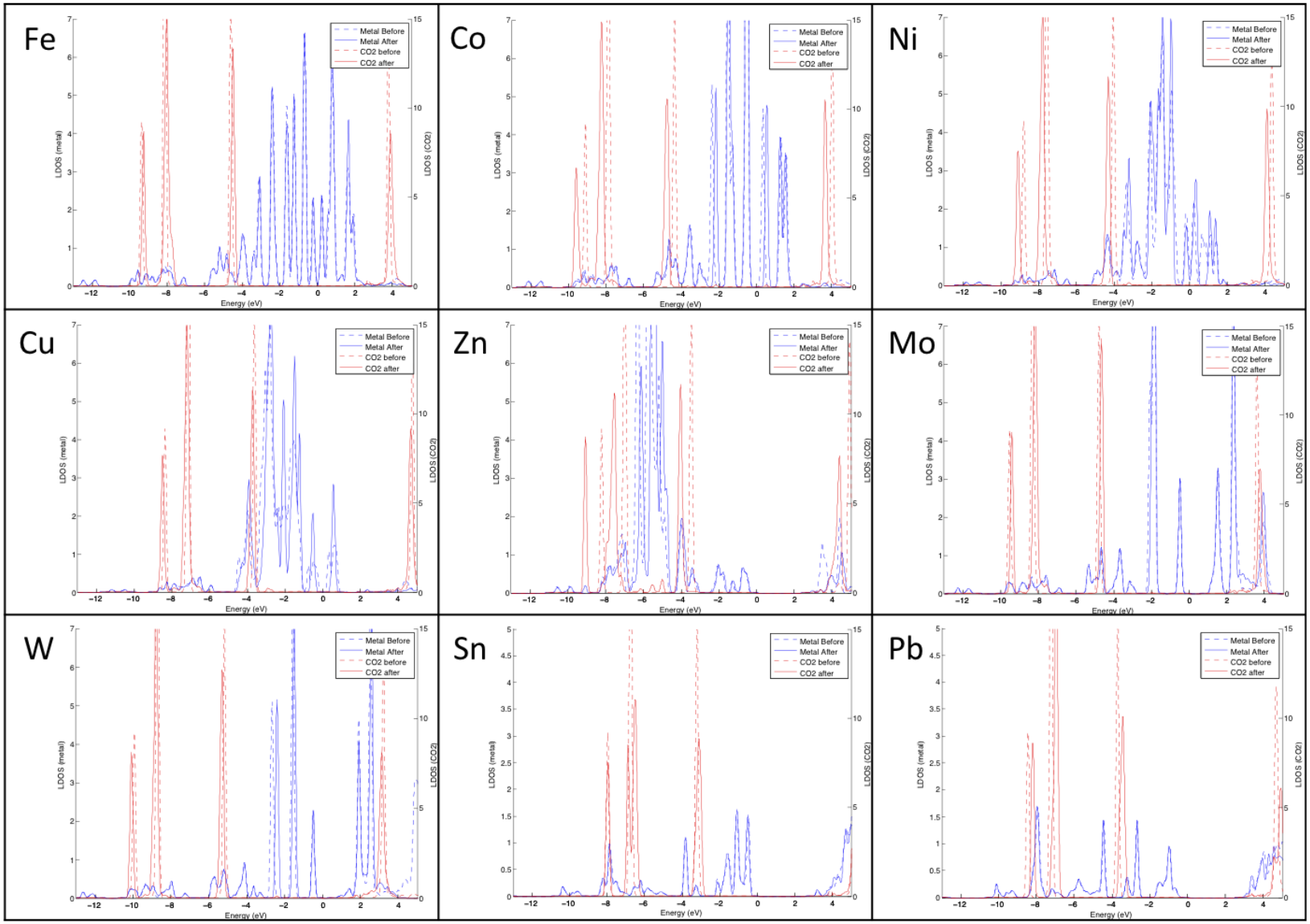

Figure S10. DOS projected to the metal site for transition metals in M-DOBDC and M-HKUST-1.

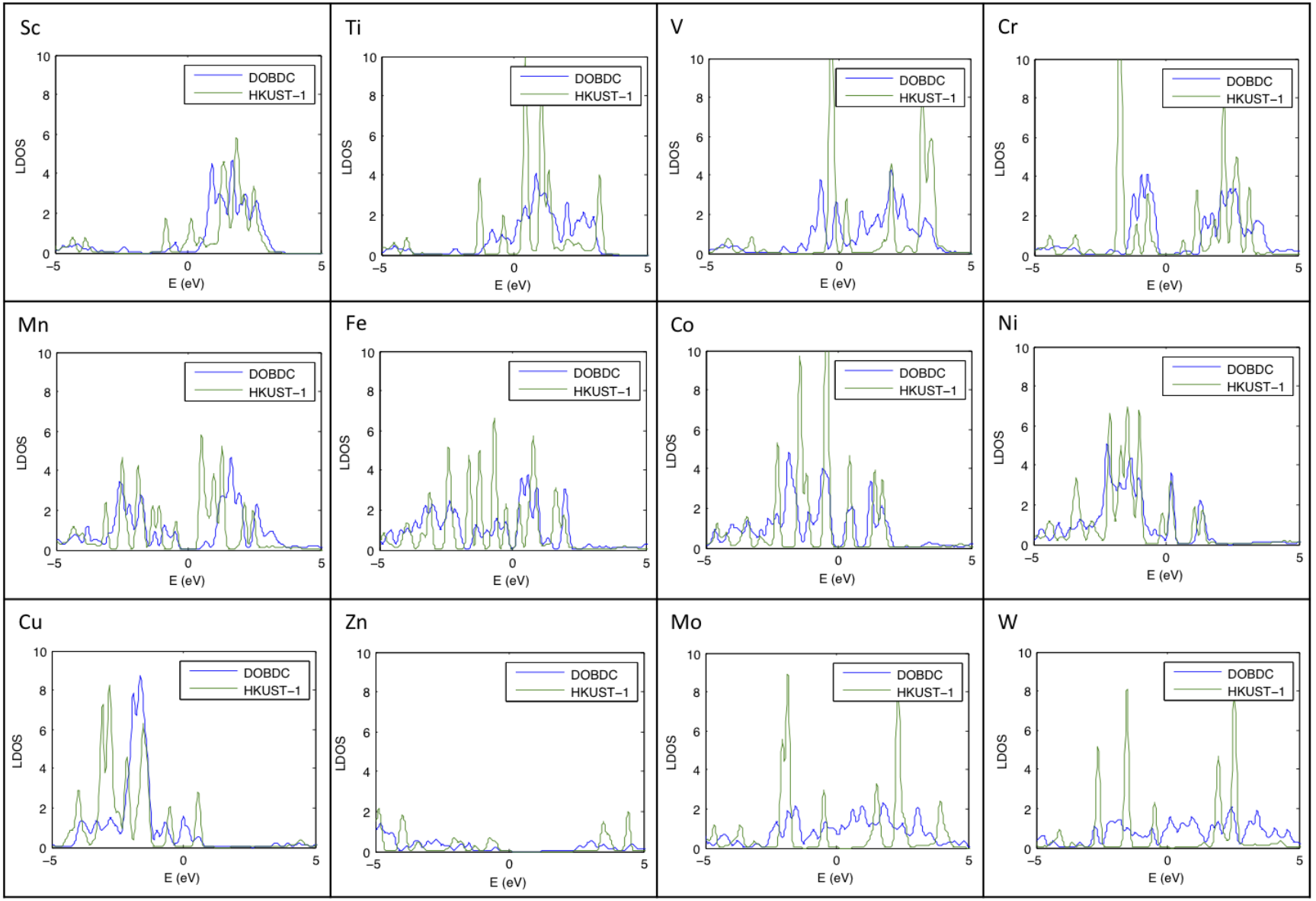

Comment regarding the geometries and energetics for M = Sn and Pb

Sn protrudes from Sn-DOBDC and Sn-HKUST-1 in a similar fashion; consequently the binding energies of these MOFs are similar. The smaller protrusion of Sn in Sn-DOBDC allows CO_2 to simultaneously interact with the ligand (carboxyl group) to give stronger binding than Sn-HKUST-1. Moreover, larger protrusion of Sn from the MOF framework results in a slight change to the CO_2 binding mode incorporating multiple-site ligand-CO_2 interactions or CO_2-CO_2 interactions. In Sn-DOBDC, CO_2 is closer to the carboxyl group and is complexed through its O atom to the C (carboxyl), with a C (carboxyl)-O_{CO2} distance of 3.562 Å. This is smaller than the Sn-O_{CO2} distance of 4.007 Å (table S5). In Sn-HKUST-1, the CO_2-CO_2 interaction influences the adsorption process. This is suggested by the shorter C_{CO2}-O_{CO2} distance, 3.177 Å, compared to the metal-CO_2 distances. This results in a change to the CO_2 orientation where C_{CO2} rather than O_{CO2} is closer to the metal. The Sn-C_{CO2} and Sn-O_{CO2} distances are, respectively, 3.783 and 3.811 Å. Thus the four-fold CUS site in Sn-DOBDC and Sn-HKUST-1influences CO_2 adsorption somewhat differently than in other metals. Behavior similar to the Sn-based compounds is found for Pb-DOBDC and Pb-HKUST-1.

Reference

1. Caskey, S. R.; Wong-Foy, A. G.; Matzger, A. J., Dramatic Tuning of Carbon Dioxide Uptake via Metal Substitution in a Coordination Polymer with Cylindrical Pores. *J. Am. Chem. Soc.* **2008,** *130* (33), 10870-10871.
2. Zhou, W.; Wu, H.; Yildirim, T., *J. Am. Chem. Soc.* **2008,** *130*, 15268.
3. Bloch, E. D.; Murray, L. J.; Queen, W. L.; Chavan, S.; Maximoff, S. N.; Bigi, J. P.; Krishna, R.; Peterson, V. K.; Grandjean, F.; Long, G. J.; Smit, B.; Bordiga, S.; Brown, C. M.; Long, J. R., Selective Binding of O2 over N2 in a Redox–Active Metal–Organic Framework with Open Iron(II) Coordination Sites. *J. Am. Chem. Soc.* **2011,** *133* (37), 14814-14822.
4. Dietzel, P. D. C.; Morita, Y.; Blom, R.; Fjellvåg, H., *Angew. Chem., Int. Ed.* **2005,** *44*, 6354.
5. Dietzel, P. D. C.; Panella, B.; Hirscher, M.; Blom, R.; Fjellvåg, H., *Chem. Commun.* **2006**, 959.
6. Sanz, R.; Martinez, F.; Orcajo, G.; Wojtas, L.; Briones, D., Synthesis of a honeycomb-like Cu-based metal-organic framework and its carbon dioxide adsorption behaviour. *Dalton Trans.* **2013,** *42* (7), 2392-2398.
7. Rosi, N. L.; Kim, J.; Eddaoudi, M.; Chen, B.; O'Keeffe, M.; Yaghi, O. M., Rod Packings and Metal−Organic Frameworks Constructed from Rod-Shaped Secondary Building Units. *J. Am. Chem. Soc.* **2005,** *127* (5), 1504-1518.
8. Murray, L. J.; Dinca, M.; Yano, J.; Chavan, S.; Bordiga, S.; Brown, C. M.; Long, J. R., Highly-Selective and Reversible O2 Binding in Cr3(1,3,5-benzenetricarboxylate)2. *J. Am. Chem. Soc.* **2010,** *132* (23), 7856-7857.
9. Maniam, P.; Stock, N., Investigation of Porous Ni-Based Metal–Organic Frameworks Containing Paddle-Wheel Type Inorganic Building Units via High-Throughput Methods. *Inorg. Chem.* **2011,** *50* (11), 5085-5097.
10. Chui, S. S.-Y.; Lo, S. M.-F.; Charmant, J. P. H.; Orpen, A. G.; Williams, I. D., A Chemically Functionalizable Nanoporous Material [Cu3(TMA)2(H2O)3]n. *Sci* **1999,** *283* (5405), 1148-1150.
11. Feldblyum, J. I.; Liu, M.; Gidley, D. W.; Matzger, A. J., Reconciling the Discrepancies between Crystallographic Porosity and Guest Access As Exemplified by Zn-HKUST-1. *J. Am. Chem. Soc.* **2011,** *133* (45), 18257-18263.
12. Kramer, M.; Schwarz, U.; Kaskel, S., Synthesis and properties of the metal-organic framework Mo3(BTC)2 (TUDMOF-1). *J. Mater. Chem.* **2006,** *16* (23), 2245-2248.
13. Shannon, R. D., Revised effective ionic radii and systematic studies of interatomic distances in halides and chalcogenides. *AcCrA* **1976,** *32* (5), 751-767.
14. Pauling, L., *The Nature of the Chemical Bond: An Introduction to Modern Structural Chemistry*. Cornell Univ: 1960.
15. Ahrens, L. H., The use of ionization potentials Part 1. Ionic radii of the elements. *Geochim. Cosmochim. Acta* **1952,** *2* (3), 155-169.